High-throughput screening of enzyme inhibition using an inhibitor gradient generated in a microchannel

Elena Garcia,[a] Melissa S. Hasenbank,[a] Bruce Finlayson[b] and Paul Yager*[a]

Received 21st June 2006, Accepted 20th September 2006
First published as an Advance Article on the web 23rd October 2006
DOI: 10.1039/b608789b

A new rapid microfluidic method for measuring enzyme inhibition is presented. The assay relies upon the creation of a uniform concentration of substrate and a microfluidically generated concentration gradient of inhibitor using a single microchannel and a single initial inhibitor concentration. The IC_{50} values of two enzyme inhibitors were determined using the new technique and validated using a conventional microtiter plate assay. Using both experimental and computational simulation techniques, the assay was shown to be sensitive to inhibitor potency and the distribution of inhibitor in the system. The method has the potential to be more accurate than conventional methods because of the comparatively large amount of data that may be collected. Recommendations for use of the assay are provided, including its use for high-throughput screening in drug discovery and general use in measurement of enzyme inhibition.

Introduction

Because drug discovery is an expensive and time-consuming process, new methods of improving its overall efficiency are in high demand. Here, we report an enzyme inhibition screening technique that has the potential to increase the throughput of one or more steps of the drug discovery process.

Enzyme inhibition assays are frequently used in drug discovery for toxicity and drug candidate screening. A typical preclinical toxicity screening method used to assess the efficacy and safety of a drug candidate involves monitoring the inhibition of the cytochrome P450 (CYPs) class of enzymes. Because these enzymes largely determine drug bioavailability, the *in vitro* inhibition of CYPs by a drug may indicate its potential to cause adverse drug interactions *in vivo*.[1–4] In addition, enzyme inhibition assays are used to screen for drug candidates that inhibit specific target enzymes involved in disease.[5–9] Current examples of such drugs include the HIV-protease inhibitors and monoamine oxidase inhibitors.

Because of their applicability, many enzyme inhibition assays have been developed.[2,10–15] These methods typically rely on either well array or microchannel systems that mix enzyme, substrate(s), and inhibitor(s) in reaction chambers, allow the reaction(s) to proceed, and measure either substrate depletion or product formation in order to determine enzyme activity. However, most current methods require the dilution of inhibitor concentrations and the sequential measurement of the enzyme activities in individual reaction chambers, which limits their amenability toward high-throughput applications.

Here, we report a novel, continuous flow microfluidic method of assaying enzyme inhibition that yields rapid, quantitative results and may be used to determine IC_{50} values. Because the assay only requires a single initial inhibitor concentration and simultaneously measures the enzyme inhibition resulting from variable inhibitor concentrations, it is well suited for high-throughput screening applications. The assay was extensively characterized using complementary experimental and computational simulation methods.

[a]*Department of Bioengineering, University of Washington, Box 355061, Foege N530J, 1705 NE Pacific Street, Seattle, WA 98195-2255, USA. E-mail: yagerp@u.washington.edu*
[b]*Department of Chemical Engineering, University of Washington, Box 355061, Foege N530J, 1705 NE Pacific Street, Seattle, WA 98195-2255, USA*

Basic principle of the assay

The assay utilized a two-inlet microfluidic device, with substrate pumped into one inlet, and the same concentration of substrate plus inhibitor pumped into the other (Fig. 1). As the two fluid streams travel through the device in the y dimension, a gradient of inhibitor forms *via* diffusion in the x dimension, while the substrate concentration remains uniform. To make the product of enzymatic activity visible, a chromogenic or fluorogenic substrate is used. After the gradient of inhibitor is established, the solution in the main channel encounters enzyme immobilized on one surface of the microchannel (the region between the dashed lines in Fig. 1), resulting in the formation of a fluorescent product. The rate of formation of product at different locations across the width of the device (in the direction of the inhibitor gradient) depends on the local inhibitor concentration. Thus, the degree of inhibition of the enzyme as a function of inhibitor concentration can be determined by monitoring the fluorophore production across x. This fluorophore production was monitored by acquiring digital images of the microchannel. A model system of an enzyme, β-galactosidase (β-gal), its fluorogenic substrate, resorufin-β-galactopyranoside[16] (RBG), and the competitive inhibitors, lactose and galactose, were used to demonstrate this assay.

To measure inhibition using the assay format described, initial velocity conditions are required. The initial velocity of an enzymatic reaction is the rate of product formation before more than about 10% of substrate has been converted to

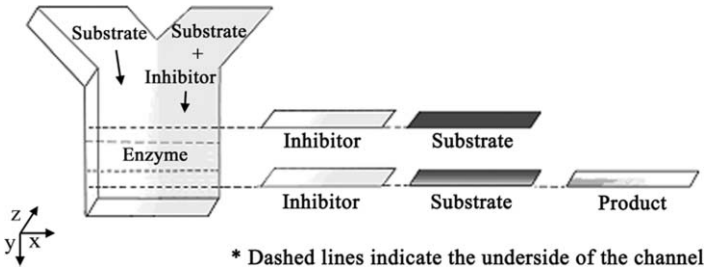

Fig. 1 Schematic of the basic principle of the assay.

product. Under initial velocity conditions, complications in analysis due to feedback inhibition and substrate concentration depletion are minimized. In the assay format as described here, initial velocity conditions are achieved since the fluid velocity in the system quickly replenishes substrate concentrations and prevents excess product accumulation. Because, under initial velocity conditions, the product concentration is directly proportional to the initial velocity, we measured product concentrations in our system in order to determine relative initial velocities.

Methods

Experimental

Microfluidic device fabrication began by patterning a solution of 333 units mL^{-1} of β-gal from *E. coli* in phosphate buffered saline (PBS), pH 7.4 (Sigma, St. Louis, MO) onto a glass slide. The slide was purchased precoated with silanes terminated in aldehyde groups (Genetix, Boston, MA) that, when exposed to protein, formed covalent bonds. Patterning was accomplished using a piezoelectric inkjet printing system (MicroFab Technologies, Inc., Plano, TX). Individual droplet volumes, on the order of 30–40 pL, were deposited onto the substrate with a 25 μm center-to-center droplet spacing. Since each droplet had a diameter of approximately 100 μm upon impact with the surface, this caused extensive droplet overlap and ensured that enzyme covered all locations across x. Patterning occurred at a relative humidity of 16% at 23 °C. A total of nine rows of spots were sequentially patterned along the length of the device; one row extended approximately seven mm in x.

The plastic layers of the device were created using a CO_2 laser cutting tool (Universal Laser Systems, Inc., Scottsdale, AZ) using methods described previously.[21] A Y-shape was cut out of 250 μm thick Mylar® doubly coated with 25 μm thick adhesive (Fralock, Canoga Park, CA), which defined the microchannel in the final device. This layer was adhered to the patterned glass slide so that enzyme spanned the width of the 6.5 mm-wide microchannel and was positioned about 7 mm downstream from the point where the two fluids merged. The exposed glass in the partially assembled device was exposed to a 10 mg mL^{-1} solution of bovine serum albumin (Sigma, St. Louis, MO) in PBS at 20 °C for 1 h. Then, the glass surface was manually rinsed with PBS containing 40 ppm Triton-X 100 (Sigma, St. Louis, MO) and submerged in the same solution. It was shaken at 20 °C for one hour in PBS with detergent, twice. After washing, the device was refrigerated overnight in the same solution. The device was then capped with a layer of 175 μm thick poly(methylmethacrylate) (GE Polymershapes, Huntersville, NC), which contained holes that corresponded to the inlets and outlet of the device. After capping, the microchannel was immediately filled with PBS containing 40 ppm Triton-X 100.

For assay operation, the device was held in a custom manifold; inlets were coupled to fluid lines (polyetheretherketone tubing, Upchurch Scientific, Oak Harbor, WA) connected to computer-controlled syringe pumps (Kloehn, Las Vegas, NV). The solution in the main channel was pumped through the device at an average fluid velocity of 74 μm s^{-1}. A Zeiss ICM-405 inverted epifluorescence microscope (Carl Zeiss Inc., Thornwood, NY) was used to monitor the fluorescence in the system. Fluorescence images during flow were captured by an integrating cooled CCD camera (Retiga 1300i *FAST*; Q Imaging, Burnaby, BC, Canada). Images were converted to intensity curves as shown in the figures using custom coded MATLAB programs (version 6.5, release 13; the MathWorks, Inc., Natick, MA). For the inhibition assays, 26 μM RBG (Molecular Probes, Eugene, OR) and the same concentration of RBG plus inhibitor were pumped through the left and right inlets of the device, respectively (Fig. 1). The different concentrations of inhibitor injected into the device for assay operation were 0.75 and 7.5 mM lactose (Sigma, St. Louis, MO) and 37.5 mM galactose (Sigma, St. Louis, MO). To obtain the uninhibited activity in the system, 26 μM RBG solutions were pumped through both sides of the device. In addition, solutions of 26 μM RBG plus 8.3 mM galactose, PBS with Triton-X 100, and 1 μM resorufin (Molecular Probes, Eugene, OR) were each pumped through both sides of the device.

The actual time of ''incubation'' for the development of the diffusion profile in a microfluidic channel like the T-sensor is not simple to determine because of the range of flow velocities present in z.[23] To calibrate the system, the diffusion of an indicator, fluorescein (Sigma Aldrich, St. Louis, MO), in PBS from one fluid stream to an adjacent fluid steam of PBS was monitored in the system using the same operational parameters as described above. The diffusion profile of fluorescein was used to estimate the effective residence time in the region of analysis used for the enzyme inhibition studies by fitting the actual profile to that predicted by a one-dimensional diffusion model created using Comsol Multiphysics (Comsol, Stockholm, Sweden) for different residence times. The effective residence time was 65 s based on the average fluid velocity in

the microchannel.

$$I_{PR} = \frac{I_S - I_B}{I_F - I_B} \quad (1)$$

The general equation used to process an image is shown in eqn (1), where I_{PR}, I_S, I_B, and I_F represent the final processed image, a sample image of fluorescent distribution, an image of flowing buffer, and a flood image of the channel filled with flowing resorufin, respectively. Processing the images in this way provided fluorescence images that accounted for the background signal from the buffer and nonuniform illumination from the fluorescence lamp. Then, the profiles across the width of the device from experimental images were found by averaging 100 pixels along y downstream from the downstream edge of the enzyme immobilization region.

Intensity profiles upstream from the enzyme immobilization region were also obtained and were used to find the background intensities in the sample profiles caused by the presence of substrate. The profiles from the sample images extracted upstream from the enzyme immobilization region in one image were subtracted from the profiles extracted downstream from the immobilization region from the same image. In order to normalize non-uniformities in enzyme density, the resulting profiles were divided by those obtained from an image of enzyme exposed to RBG only across x.

The diffusion profiles of inhibitor in the system were calculated by fitting experimentally determined values to diffusion profiles obtained from simulations. Since the normalized inhibitor concentration of 0.5 for all diffusion profiles was in the same location, the location of the normalized inhibitor concentration of 0.5 was found using the profile of fluorescein diffusion. Then, for each inhibitor profile, the location of an additional inhibitor concentration in x was determined by finding the location of the product concentration in the assay data caused by a known concentration of inhibitor and assigning that location to the known concentration of inhibitor. In this way, two inhibitor concentration locations were found, which were then fitted to a one-dimensional diffusion model using Comsol Multiphysics by changing the diffusion coefficient.

For the conventional microtiter plate method, the inhibition caused by one inhibitor was monitored using two rows of a polystyrene 96-well plate—one replicate for each row. The wells in columns 11 and 12 were filled with 200 μL of buffer and RBG respectively. The wells in column 10 were filled with 180 μL of RBG. Then, stock inhibitor concentrations of either 16 mM lactose or 80 mM galactose were serially diluted in columns 1–9. Next, enzyme was placed into wells 1–10, and the plate was incubated at 20 °C for 15 min. The reaction was arrested by placing the plate in an oven at 80 °C for 5 min. After the plate was allowed to cool, the product concentration in each well was measured using the well plate reader accessory of a fluorometer (Luminescence Spectrometer LS50B, Perkin Elmer, Wellesley, MA). The fluorescence intensities in each of the columns were averaged along the rows of the plate. The averaged fluorescence intensity from column 11 was subtracted from the averaged intensities from columns 1–10. Then, the resulting values in columns 1–9 were normalized by column 10 to yield fractional initial velocity measurements.

For the conventional microtiter plate assay, β-gal activity in the presence of lactose and galactose was monitored using a polystyrene 96-well plate. All solutions were made using PBS at a pH of 7.4. An inhibitor, in the presence of 26 μM RBG, was serially diluted into nine wells of the plate. An addition well was filled with 26 μM RBG without inhibitor. Then, enzyme was introduced to the filled wells, and the plate was incubated at 20 °C for 15 min. The reaction was arrested by placing the plate in an oven at 80 °C for 5 min. After the plate was allowed to cool, the product concentration in each well was measured using the well plate reader accessory of a fluorometer (Luminescence Spectrometer LS50, Perkin Elimer, Wellesley, MA). The fractional enzyme activities or initial velocities caused by the variable inhibitor concentrations were found by normalizing the product intensity at a particular inhibitor concentration by the product intensity of the uninhibited case. Duplicate measurements were made for each inhibitor concentration.

Statistical analysis

To obtain IC_{50} values from the microfluidic and conventional data, the initial velocities were plotted *versus* inhibitor concentration. For the microfluidic data, standard linear regression with a quadratic term was fitted to the data on a restricted range of inhibitor concentrations that was associated with values of normalized fluorescence slightly above and slightly below the IC_{50} value (n = 16 for lactose, n = 23 for galactose). A bootstrap statistical procedure[24] was used to estimate IC_{50}, as well as the corresponding standard errors, by resampling the residuals from the fitted regression model. The bootstrap procedure was used because the fit of the theoretical non-linear model showed systematic structure in the error terms, calling into question the validity of the estimates obtained from standard modeling techniques. An identical statistical procedure was used with the conventional data (n = 5 for lactose, n = 7 for galactose) to obtain IC_{50} values. The differences between the IC_{50} values obtained using the two methods were not statistically different than zero (two-sided test, p = 0.214 for lactose, p = 0.372 for galactose).

Computational simulation

A three-dimensional simulation of the enzyme inhibition assay was created using Comsol Multiphysics. The model geometry was obtained from experimental devices. The Navier–Stokes and convection-diffusion equations were used to simulate fluid motion and the mass transport of substrate, inhibitor, and product, respectively. The constants and variables for this model were obtained from published or experimental values (Table 1). The rate of product formation in the system equaled the rate of substrate depletion. The Reynolds number (defined as the product of the density of water, the average fluid velocity in the main channel, and the characteristic length (depth of the device) divided by the viscosity of water) was 0.02. The Peclet numbers (defined as the product of the average fluid velocity and the characteristic length divided by the diffusivity of the chemical species in water) for product and

Table 1 Constants and expressions used in the simulation. 'E', 'S', 'I', and 'P' correspond to enzyme, substrate, inhibitor, and product, respectively. 'R' corresponds to the rate of product formation and was based on standard Michaelis–Menten kinetics for competitive inhibition

Name	Variable	Value or expression
Characteristic length or depth of device	x_S	0.3 mm (from experiment)
Average fluid velocity	u_S	0.074 mm s^{-1} (from experiment)
Diffusivity of RBG	D_S	4.3×10^{-4} mm^2 s^{-1} [22]
Diffusivity of lactose	D_l	6.6×10^{-4} mm^2 s^{-1} for lactose or 16×10^{-4} mm^2 s^{-1} for galactose (from experimental fit)
Diffusivity of resorufin	D_P	6.6×10^{-4} mm^2 s^{-1} [22]
Michaelis constant	K_M	4.5×10^{-4} M
Characteristic substrate concentration	S_0	26×10^{-5} M (from experiment)
Characteristic inhibitor concentration	I_0	75, 7.5, or 0.75 mM lactose or 37.5 mM galactose (from experiment)
Kinetic rate constant	K_2	77.2 s^{-1} (calculated using data not shown)
Inhibition constant	K_I	0.760 mM for lactose or 12.4 mM for galactose (from a least square fit of experimental data)
Kinetic rate constant for lactose	K_2^1	103.34 s^{-1} (derived[25])

Table 2 Boundary conditions for the Navier–Stokes (N-S) and convection–diffusion (C–D) equations. 'C' represents the concentration of respective chemical species, while 'R' and 'R_2' represent the reaction rates for the depletion of substrate or formation of product and the depletion of inhibitor, respectively

Boundary	N–S	C–D substrate	C–D inhibitor	C–D product
Substrate and inhibitor inlet	$x = 0$ $y = 6z(1 - z)$ $z = 0$	$C = 1$	Mapped from 2D simulation	$C = 0$
Enzyme patch	No slip	Flux $= -R$	Flux $= -R_2$	Flux $= R$
Outlet	Normal flow/pressure	Convective flux	Convective flux	Convective flux
All others	No slip	Insulation	Insulation	Insulation

lactose, galactose, and substrate were 52, 34, and 14, respectively. The boundary conditions for the model are displayed (Table 2). The initial fluid velocities in the *x*-, *y*-, and *z*-directions were one, zero, and zero, respectively. The initial concentrations in the entire model geometry for substrate, inhibitor and product were one, zero, and zero, respectively.

To reduce the size of the three-dimensional model, a separate two-dimensional, *x*–*z* model was used to simulate the diffusion of inhibitor from one fluid stream to another upstream from the enzyme immobilization area. The two-dimensional geometry corresponded experimentally to the area of the device after the two fluid streams merged and before the enzyme patch. The Poisson and the pseudo-three-dimensional convection–diffusion equations were used to simulate the fluid velocity and transport of lactose, respectively. The pseudo-three-dimensional convection-diffusion equation neglected diffusion in *y*. For the Poisson equation, the maximum velocity in the microchannel was a normalized value of 1.5, and Dirichlet boundary conditions were imposed on the walls so that the fluid velocity at the walls of the simulated microchannel was zero. For the pseudo-three-dimensional convection-diffusion equation, the diffusivity of lactose and the normalized fluid velocity from the Poisson equations were used to solve the model. Insulation conditions (the flux perpendicular to the walls was zero) were imposed on the walls of the microchannel. The initial concentration of inhibitor on one half of the geometry was one, while it was zero on the remaining half. After first solving the Poisson equation, the resulting solution was used to solve the convection-diffusion equation for 47 seconds. The resulting distribution of inhibitor was then mapped onto the inlet of the three-dimensional model geometry and was used as a boundary condition (Table 2).

To solve the steady-state three-dimensional model, the steady-state Navier–Stokes and convection–diffusion equations were solved simultaneously. The initial inhibitor concentrations used are shown (Table 1). The product and inhibitor concentrations obtained from the final solved model at the outlet of the model geometry were summed through *z* at 100 points across *x*. This manner of data analysis allowed direct comparison to experimental fluorescence data taken from top-view perspectives.

Additionally, model parameters were examined by changing the diffusion coefficient of inhibitor or K_I for an initial lactose concentration of 7.5 mM. Additional diffusion coefficients of inhibitor evaluated were 2.2×10^{-6} and 19.8×10^{-6} cm^2 s^{-1}, while additional K_I values were 0.19 and 3.040 mM.

Results

The experimental initial velocities and inhibitor distributions across *x* for initial inhibitor concentrations of 7.5 mM lactose and 37.5 mM galactose are shown (Fig. 2 A); these profiles were extracted from experimental processed images. The initial velocities were also plotted *versus* the corresponding inhibitor concentrations (Fig. 2 B). The standard deviations of 100 pixels in *y* at corresponding *x* values are illustrated.

Lactose was found to be a more potent inhibitor of β-gal activity than galactose (Fig. 2). The IC_{50} values and standard errors determined for inhibition by lactose and galactose using the microfluidic method were 0.6756 ± 0.0021 (95% CI: 0.6719, 0.6799) and 12.02 ± 0.0182 (95% CI: 11.98, 12.06) mM, respectively, while the IC_{50} values and standard errors found for inhibition by lactose and galactose using a conventional plate method were 0.7119 ± 0.0408 (95% CI: 0.6429, 0.7865) and 13.15 ± 0.9099 (95% CI: 11.67, 15.11) mM,

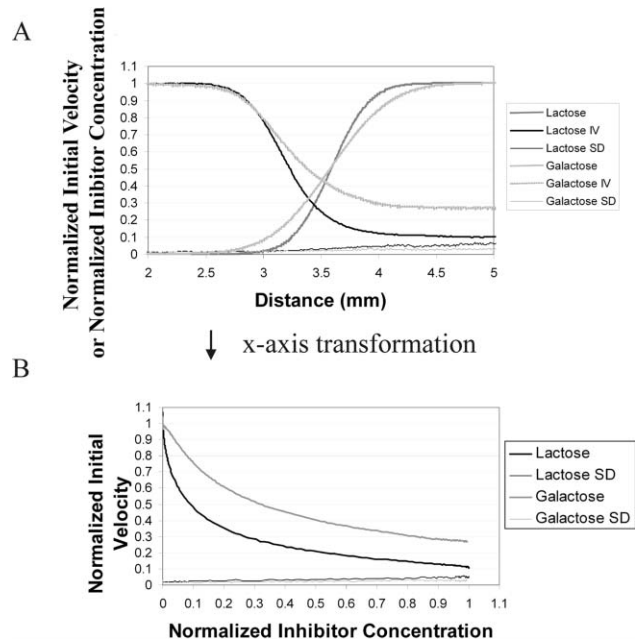

Fig. 2 Experimental data displayed as a function of distance along x (A) and the normalized inhibitor concentration (B). In A, the inhibitor distribution is indicated by the inhibitor name. The corresponding initial velocities and standard deviations associated with an inhibitor are indicated by the inhibitor name followed by IV and SD, respectively. In B, the corresponding initial velocities and standard deviations associated with an inhibitor are indicated by the inhibitor name and the inhibitor name followed by SD, respectively. The concentrations of lactose and galactose in the system were normalized by 7.5 and 37.5 nM, respectively.

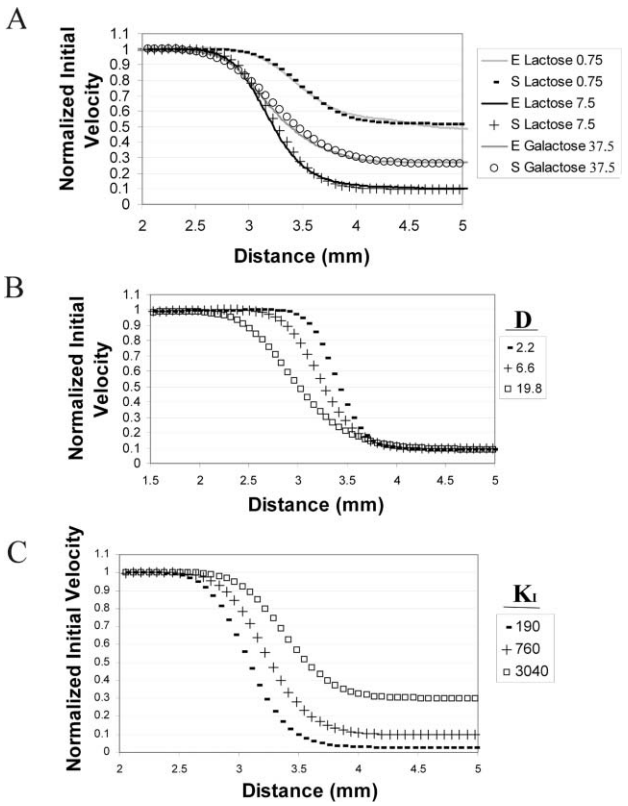

Fig. 3 Computational simulation results. Comparison of normalized initial velocities obtained from experiments and simulations (A). In the legend, E and S indicate experimental and simulation results, respectively. The concentrations of lactose used in mM are indicated, and the concentration of galactose used was 37.5 mM. Model results of lactose inhibition using various diffusivities of inhibitor in units of 10^{-6} cm^2 s^{-1} (B) and K_I values in units of μM (C). For all graphs, at intermediate inhibitor concentrations, the concentration of inhibitor increased with increasing x.

respectively. The differences in the IC_{50} values between the conventional and microfluidic methods were not statistically significant at the 0.05 level.

The profiles of product and inhibitor concentrations extracted from experiments and simulations are illustrated (Fig. 3 A). Similar trends were observed experimentally and in simulations for different initial concentrations of inhibitor. When the initial concentration of lactose was 0.75 mM, or near the IC_{50} value, the minimum fractional initial velocity obtained was approximately 0.5, as expected. With an initial lactose concentration of 7.5 mM, or about ten times the IC_{50} value, a maximum initial velocity of about 0.1 was found and a greater range of inhibition was achieved compared to when the lower concentration of inhibitor was used. In addition, agreement between the simulation and experimental results was observed with an initial galactose concentration of 37.5 mM, which had a different K_I than that used for the lactose simulations.

As the experimental data validated the simulations, the model was used to explore the effect of inhibitor distribution in the system by changing its diffusion coefficient (Fig. 3 B). The initial velocities were calculated using the actual diffusion coefficient of lactose (6.6×10^{-6} cm^2 s^{-1}), as well as ⅓ and 3 times this value. Since the substrate concentration, K_M, and K_I values in each condition were identical, the IC_{50} values for each of the conditions were equivalent. As expected, since the inhibitor concentration was identical for all conditions at the highest and lowest inhibitor concentrations, the initial velocities resulting from exposure to these concentrations were equivalent. However, since the diffusion-driven distribution of inhibitor in the system for each condition was different at intermediate concentrations, the initial velocities corresponding to these concentrations were also distributed differently. As shown, the lowest diffusion coefficient caused the narrowest initial velocity profile, while the highest diffusion coefficient caused the broadest initial velocity profile, which caused corresponding shifts in the location of 50% inhibition even though the IC_{50} values were identical.

The models were also sensitive to the potency of the inhibitor or K_I (Fig. 3 C). The distribution of inhibitor, substrate concentration, and K_M values were identical for each condition, while the K_I values varied from its approximate actual value of 760 μM to ¼ and 4 times this value. Therefore, the IC_{50} values were proportional to K_I. As expected, at all normalized initial velocities of less than one, the lowest and highest K_I conditions resulted in relatively better and worse inhibition, respectively. For each condition, this caused corresponding shifts in the location of 50% inhibition even though the inhibitor distributions were identical.

Discussion

The microfluidic assay described here has several advantages compared to traditional microtiter plate methods. In our hands, the plate assay required over 15 min—a typical duration for such assays, but the microfluidic enzyme inhibition assay took only about 2 min. Compared to microtiter plate methods, the microfluidic method was also simpler to operate since it required only one initial inhibitor concentration, which was diluted within the device. Additionally, instead of recording measurements from individual wells, this new assay allowed the simultaneous measurement of enzyme activity at a range of inhibitor concentrations. Finally, because the microfluidic method provided initial velocity measurements from 40–50-fold higher inhibitor concentrations and 50 times more measurements were made at each inhibitor concentration compared to the conventional method, the standard errors for the kinetic values in the microfluidic data were substantially lower than those for the plate data.

The standard errors for the microfluidic assay were estimated using the bootstrap method based on the error found from 100 pixels in one column of an image corresponding to one inhibitor concentration. The error in the pixel column took into account the product and inhibitor diffusion that occurred within the pixel column; it also took into account flow instabilities due to the pulsatile flow in our system, which occurred at a rate of 138 Hz. Since the diffusion profile of a fluorescence indicator in the system was stable over time and enzyme damage in the presence of substrate upon exposure to fluorescence excitation was observed, only one image for each inhibitor was taken. The values determined in this report were consistent with other similar experiments performed in different devices.

In general, in order to extract IC_{50} values using the reported method, the distribution of inhibitor in the system must be determined. Since the method of determining inhibitor distribution used here depended largely on diffusion, conditions that complicate inhibitor diffusion should be avoided. For instance, the viscosities and densities of the two solutions placed into the device should be similar. Differences in viscosity could lead to the uneven occupation of the two fluid streams within the device,[17] while differences in density could cause gravity-induced reorientation of the fluids.[18] Both of these factors would make it difficult to determine inhibitor distributions. If changes in the properties of one solution placed into the device are unavoidable, properties in the other solution should be correspondingly matched. This could be done, for instance, by the addition of molecules to one solution that change its properties but that do not interfere with the enzymatic reaction.

In order to directly measure IC_{50} values, the initial concentration of inhibitor placed in the device must be greater than the IC_{50}, otherwise 50% inhibition will not be realized. However, if the initial concentration of inhibitor is much greater than the IC_{50} value, product concentrations corresponding to variable levels of inhibition will be restricted to relatively fewer pixel columns in x. As a general guideline, to avoid these problems, initial inhibitor concentrations should be in a range from two to ten times the IC_{50} value, which could be estimated by performing preliminary assays with variable initial inhibitor concentrations.

The flow rates used in the assays were chosen in order to create a distribution of inhibitor in the system that ranged from zero to the initial inhibitor concentration placed in the device. Additionally, the diffusion profile of inhibitor was chosen so that it was sufficiently broad over the imaging region so that the gradient, across the width of the device, spanned several pixel columns allowing resolution of the inhibitor concentrations that caused 50% inhibition of the enzyme. At relatively high flow rates, the inhibition diffusion profile would be steep, spanning relatively fewer pixel columns. Compared to a relatively broader inhibitor diffusion profile, this would result in a less precise determination of the IC_{50} value since the pixel column corresponding to 50% inhibition of the enzyme would correspond to a wider range of inhibitor concentrations.

In addition, in this study, measurements were made of the IC_{50} values of competitive inhibitors, which compete with substrate for the active sites of the enzyme. Because relatively high concentrations of substrate in the system would reduce the effect of the inhibitor and make it difficult to observe, the substrate concentration used in the assay were less than the K_M of the substrate.

While demonstrated for one model enzyme system, this assay could be applied toward a wide range of enzyme systems. For direct use of the assay, a fluorogenic or colorimetric substrate must be available and the rate of product formation must be high enough to ensure a detectable product signal near the enzyme immobilization region before significant interdiffusion of the reactant(s) or product(s) occurs. For enzyme systems with slow reaction times, a range of inhibitor concentrations in individual microchannels could be created using a similar Y-shaped channel and splitting its outlet into a series of smaller channels.[19] The reactions could then proceed for relatively longer periods of time without the product and inhibitor diffusion that would occur in the system as presented. The wide range of continuous and discontinuous gradients that can be produced by microfluidic devices[20] would allow the assay developed here to be fine-tuned for particular types of inhibition. While a wide range of fluorogenic substrates are available,[21] radioactive, spectroscopic, or amperometric methodologies could also be used in the assay by implementing the corresponding detection systems. With the modifications suggested, the assay reported here could be highly versatile, accommodating enzyme systems with slow turnover rates and/or systems without available fluorogenic substrates.

Acknowledgements

E. G. and M. S. H. would like to acknowledge the financial support of the Singapore–University of Washington Alliance (SUWA) funded by Singapore's Biomedical Research Council's Agency for Science, Technology and Research (A*STAR) and the NIDCR (Grant No. T32-DE07023), respectively. Support was also provided from the Washington Technology Center at the University of Washington. In addition, we thank Dr Patrick Stayton, Dr Anson Hatch, Dr Noah Malmstadt, Kristen Helton, Paolo

Spicar-Mihalic, Jennifer Foley, and Dr Thayne Edwards for their helpful discussions and contributions regarding this work.

References

1 C. L. Crespi, V. P. Miller and B. W. Penman, Microtiter plate assays for inhibition of human, drug-metabolizing cytochromes P450, *Anal. Biochem.*, 1997, **248**, 188–190.

2 C. L. Crespi, V. P. Miller and D. M. Stresser, Design and application of fluorometric assays for human cytochrome P450 inhibition, *Methods Enzymol.*, 2002, 276–284.

3 K. M. Jenkins, R. Angeles, M. T. Quintos, R. Xu, D. B. Kassel and R. A. Rourick, Automated high throughput ADME assays for metabolic stability and cytochrome P450 inhibition profiling of combinatorial libraries, *J. Pharm. Biomed. Anal.*, 2004, **34**, 989–1004.

4 A. A. Nomeir, C. Ruegg, M. Shoemaker, L. V. Favreau, J. R. Palamanda, P. Silber and C.-C. Lin, Inhibition of CYP3A4 in a rapid microtiter plate assay using recombinant enzyme and in human liver microsomes using conventional substrates, *Drug Metab. Dispos.*, 2001, **29**, 748–753.

5 S. Gulnik, J. W. Erickson and D. Xie, HIV protease: Enzyme function and drug resistance, *Vitam. Horm.*, 2000, **58**, 213–256.

6 L. V. Gubareva, R. G. Webster and F. G. Hayden, Detection of influenza virus resistance to neuraminidase inhibitors by an enzyme inhibition assay, *Antiviral Res.*, 2002, **53**, 47–61.

7 L. M. Benson, K. A. Veverka, D. C. Mays, A. N. Nelson, Z. H. Shriver, J. J. Lipsky and S. Naylor, Simultaneous structure—activity determination of disulfiram photolysis products by on-line continuous-flow liquid secondary ion mass spectrometry and enzyme inhibition assay, *J. Chromatogr., A*, 1995, **693**, 162–166.

8 F. H. Clarke, *How Modern Medicines Are Discovered*, Futura Publishing Company, Mount Kisco, NY, USA, 1973.

9 V. Vermeirssen, J. Van Camp and W. Verstraete, Optimization and validation of an angiotensin-converting enzyme inhibition assay for the screening of bioactive peptides, *J. Biochem. Biophys. Methods*, 2002, **51**, 75–87.

10 A. R. de Boer, B. Bruyneel, J. G. Krabbe, H. Lingeman, W. M. A. Niessen and H. Irth, A microfluidic-based enzymatic assay for bioactivity screening combined with capillary liquid chromatography and mass spectrometry, *Lab Chip*, 2005, **5**, 1286–1292.

11 J. Dunne, H. Reardon, V. Trinh, E. Li and J. Farinas, Comparison of on-chip and off-chip microfluidic kinase assay formats, *Assay Drug Dev. Technol.*, 2004, **2**, 121–129.

12 A. G. Hadd, S. C. Jacobson and J. M. Ramsey, Microfluidic assay of acetylcholinesterase inhibitors, *Anal. Chem.*, 1999, **71**, 5206–5212.

13 A. G. Hadd, D. E. Raymond, J. W. Halliwell, S. C. Jacobson and J. M. Ramsey, Microchip device for performing enzyme assays, *Anal. Chem.*, 1997, **69**, 3407–3412.

14 P. Kotturi and M. Boudreau, Mobility shift screening assays for protein kinase targets, *Am. Lab.*, February 2003, 32–39.

15 A. Pommereau, E. Pap and A. Kannt, Two simple and generic antibody-independent kinase assays: comparison of a bioluminescent and a microfluidic assay format, *J. Biomol. Screening*, 2004, **9**, 409–416.

16 J. Hofmann and M. Sernetz, Immobilized enzyme kinetics analyzed by flow-through microfluorimetry, *Anal. Chim. Acta*, 1984, **163**, 67–72.

17 A. E. Kamholz, E. A. Schilling and P. Yager, Optical measurement of transverse molecular diffusion in a microchannel, *Biophys. J.*, 2001, **80**, 1967–1972.

18 S. K. Yoon, M. Mitchell, E. R. Choban and P. J. Kenis, Gravity-induced reorientation of the interface between two liquids of different densities flowing laminarly through a microchannel, *Lab Chip*, 2005, **5**, 1259–1263.

19 M. A. Holden, S. Kumar, E. T. Castellana, A. Beskok and P. S. Cremer, Generating fixed concentration arrays in a microfluidic device, *Sens. Actuators, B*, 2003, **92**, 199–207.

20 D. Irimia, D. A. Geba and M. Toner, Universal micro-fluidic gradient generator, *Anal. Chem.*, 2006, **78**, 3472–3477.

21 J.-P. Goddard and J.-L. Reymond, Recent advances in enzyme assays, *Trends Biotechnol.*, 2004, **22**, 363–370.

22 E. A. Schilling, A. E. Kamholz and P. Yager, Cell lysis and protein extraction in a microfluidic device with detection by a fluorogenic enzyme assay, *Anal. Chem.*, 2002, **74**, 1798–1804.

23 A. E. Kamholz, B. H. Weigl, B. A. Finlayson and P. Yager, Quantitative analysis of molecular interaction in a microfluidic channel: the T-sensor, *Anal. Chem.*, 1999, **71**, 5340–5347.

24 A. R. Henderson, The bootstrap: A technique for data-driven statistics. Using computer-intensive analyses to explore experimental data, *Clin. Chim. Acta*, 2005, **359**, 1–26.

25 C. C. Pessela, C. Mateo, M. Fuentes, A. Vain, J. L. Garcia, A. V. Carrascosa, J. M. Guisan and R. Fernandez-Lafluente, Stabilization of a multimeric beta-galactosidase from Thermus sp. strain T2 by immobilization on novel heterofunctional epoxy supports plus aldehyde–dextran cross-linking, *Biotechnol. Prog.*, 2004, **20**, 388–392.